Astronomy & Astrophysics manuscript no.
(will be inserted by hand later)

Simultaneous single-pulse observations of radio pulsars

I. The polarization characteristics of PSR B0329+54

A. Karastergiou[1], A. von Hoensbroech[1], M. Kramer[2], D. R. Lorimer[3], A. G. Lyne[2], O. Doroshenko[1], A. Jessner[1], C. Jordan[2], and R. Wielebinski[1]

[1] Max-Planck Institut für Radioastronomie, Auf dem Hügel 69, 53121 Bonn, Germany
[2] Jodrell Bank Observatory, University of Manchester, Macclesfield, Chesire SK11 9DL, UK
[3] Arecibo Observatory, HC3 Box 53995, Arecibo, Puerto Rico, PR 00612, USA

the date of receipt and acceptance should be inserted later

Abstract. We present the first results from a programme of multi-frequency simultaneous single pulse observations carried out as part of the European Pulsar Network. We detail the main data analysis methods and apply them to simultaneous observations of the strong pulsar B0329+54 at 1.4 and 2.7 GHz using the Jodrell Bank and Effelsberg radio telescopes respectively. The pulses at different frequencies are highly correlated in their total intensity, as seen in previous experiments, and generally show consistent position angles of the linearly polarized component. In contrast, the circularly polarized emission sometimes shows clear differences between pulses received at different frequencies. These results are unexpected and warrant further follow-up studies to interpret them in the context of the intrinsic bandwidth of pulsar radiation.

Key words. pulsars: PSR B0329+54; single-pulses; emission mechanism – polarization

1. Introduction

Despite significant observational and theoretical progress since the discovery of pulsars in 1968, there is still considerable uncertainty surrounding the detailed physics of the emission process responsible for the radio pulses observed in the spectrum between 50 MHz all the way up to 90 GHz (see Melrose 2000 for a review). Although much of what we understand has been gleaned from studies of integrated pulse profiles, further understanding of the observed emission from radio pulsars is perhaps best tackled by studying individual pulses and their behaviour with time. Any satisfactory theory of emission has to be able to explain the following observed properties:

- moding, drifting and nulling: the relevant phenomena here are the pulse-to-pulse patterns that consist of the pulsar profile changing, sub-components of the profile drifting across the pulse or the pulse disappearing altogether for several periods.
- microstructure: features seen in the pulse on very small time scales ($\lessapprox 1$ ms)
- orthogonal polarization modes: here the polarization position angle executes a jump at certain pulse longitudes, which is often close to 90^o.

For further information on these phenomena, see Lyne and Smith (1998) and references therein.

In the past, a number of experiments have been conducted to investigate the multi-frequency properties of individual pulses of radio pulsars (see e.g. Bartel & Sieber 1978, Boriakoff et al. 1981, Bartel et al. 1981, Davies et al. 1984, Kardashev et al. 1986 and Sallmen et al. 1999). Most of these observations studied total power only and addressed questions concerning the bandwidth of the emission, the correlation of microstructure and the validity of the cold plasma dispersion law for pulsars. Bartel & Sieber (1978) simultaneously observed individual pulses of PSR B0329+54 and PSR B1133+16 at 0.3 and 2.7 GHz, using the Effelsberg radio telescope. The correlation coefficients of the time series of the pulse energies at the two different frequencies are found to be around 75%, indicating a broadband nature of the emission. Simultaneous observations between the Pushchino BSA transit array at 0.1 GHz and the Effelsberg radio telescope at 1.7 GHz were presented by Bartel et al. (1981) (PSR B0809+74) and Kardashev et al. (1986) (PSR B0329+54, PSR B0834+06, PSR B1133+16, PSR B1508+55). Bartel et al. (1981) also showed that nulling occured simultaneously at both frequencies at 0.10 and 1.70 GHz for PSR B0809+74. Simultaneous observations of the same pulsar by Davies et al. (1984) at 0.10 GHz, 0.41 GHz and 1.41 GHz using the Lovell telescope at Jodrell Bank and the BSA array showed that nulls at 0.4 GHz always corresponded to nulls at 0.1 GHz, but not vice versa. Finally, Sallmen et al.

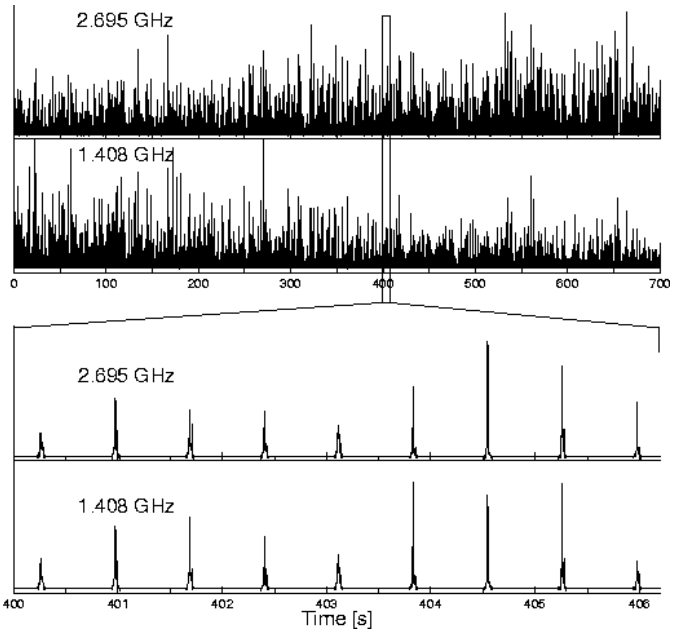

Fig. 1. Total power time series of single pulses of PSR B0329+54 measured at 1.4 GHz (Jodrell Bank) and 2.7 GHz (Effelsberg). Top two panels show an 11-min long interval. The long time scale intensity variations between the two telescopes are caused by interstellar scintillation. Bottom two panels show a close-up of a few pulses. Off-pulse regions have been zeroed for clarity. A very good overall correlation is obvious.

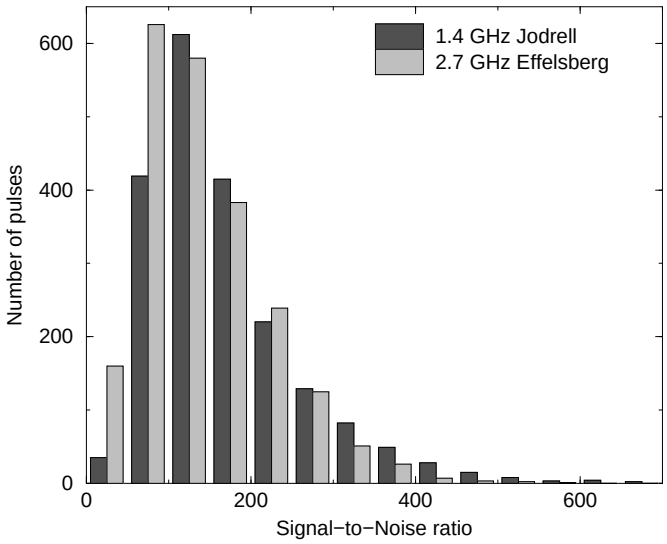

Fig. 2. Signal-to-noise ratio distributions of 1912 simultaneously recorded single pulses of PSR B0329+54 between Jodrell Bank (1.4 GHz) and Effelsberg (2.7 GHz). The high quality of the data allows a polarimetric investigation of the pulses.

(1999) simultaneously observed giant pulses of the Crab pulsar at 1.4 GHz at the VLA and 0.6 GHz in Green Bank. About 70% of the giant pulses are seen at both 1.4 and 0.6 GHz, implying a broad emission mechanism bandwidth.

In 1995, a large scale project was launched by the European Pulsar Network. Simultaneous observations of individual pulses were conducted between various collaborating observatories across Europe and the world (Effelsberg, Jodrell Bank, Bologna, Westerbork, Puchshino, Ooty, Torun, Arecibo), as individual experiments. The data presented in this paper were obtained during such a polarimetric experiment between the Jodrell Bank and Effelsberg radio telescopes observing at the frequencies of 1.41 GHz and 2.70 GHz, respectively. In this paper, we concentrate on the strong pulsar B0329+54 to introduce our methods which will be also used in future studies.

In addition to being one of the strongest pulsars in the sky, and therefore ideal for single-pulse observations, PSR B0329+54 exhibits many of the typical pulsar emission features which are not well understood. Its profile consists of a core component and at least four conal outriders surrounding it (e.g. Kramer 1994). The most striking feature is perhaps its mode changing property (Lyne 1971, Bartel et al. 1982), which is observed at frequencies as high as 32 GHz and 43 GHz (Kramer et al. 1997). The average profile shows significant amounts of linear and circular emission across the whole pulse. The position angle (PA) of the average linearly polarized emission shows frequent orthogonal jumps resulting from orthogonal polarization modes (OPMs) which are probably simultaneously present (e.g. McKinnon & Stinebring 1998). Indeed, the seemingly complicated PA swing was finally unravelled by Gil & Lyne (1995) who used single pulse observations at 0.4 GHz to separate the PA swing in two different curves representing each OPM.

Despite being studied so well, simultaneous multi-frequency observations of PSR B0329+54 with full polarization information were still missing. Since such observations are essential to distinguish between emission properties caused by propagation effects (in the pulsar magnetosphere) or those intrinsic to the emission process (cf. Melrose 1995), B0329+54 is an excellent source to begin such a study which is the subject of the rest of this paper. In §2 we give details about the observations and the telescopes involved, before we describe the data reduction in §3. The results are presented in §4 and discussed in §5. We summarize the main conclusions in §6 and give an outlook onto further studies in §7.

2. Observations

A sequence of 1912 pulses of very good signal-to-noise ratio (S/N) were recorded simultaneously between the 76-m Lovell radio telescope at Jodrell Bank at 1.408 GHz and the 100-m Effelsberg radio telescope at 2.695 GHz, on the 13^{th} of July, 1997. A dual-channel cryogenic receiver was used on the Lovell telescope, sensitive to both senses of circular polarization. The system equivalent flux density was 37 Jy. A 2×32-channel filterbank was used, producing all 4 Stokes parameters for each 1-MHz wide channel, before data were de-dispersed in hardware for

off-line processing. The effective time resolution was 158 μs. The Effelsberg data were recorded using a cooled receiver with HEMT amplifiers providing two circular polarizations with a bandwidth of 80 MHz and a system equivalent flux density of 2.7 Jy. Given the pulsar's dispersion measure of 26.776 cm^{-3}pc, the smearing time across the whole bandwidth was 909μs, compared to a sampling time of 550 μs. Stokes parameters were formed for the full 80 MHz and transferred to disk.
In order to calibrate the data, both telescopes perform observations of standard unpolarized continuum sources of known flux density together with the signal of a switched linearly polarized signal injected into the feeds, as described for Effelsberg by von Hoensbroech & Xilouris (1997) and for Jodrell Bank by Gould & Lyne (1998). The average S/N at both observatories was between 100 and 200, with hardly any pulses below 30 (see Fig. 2).

3. Data analysis

Several simultaneous multi-frequency observations of individual pulses were made on PSR B0329+54 and a number of other pulsars, which will be described here and in subsequent papers. The data format, starting time of the observations and time resolution usually differ between the different telescopes. Therefore the raw data were calibrated and converted into the common EPN-format (Lorimer et al. 1998). Subsequently, a procedure described below was used, which aligns and re-bins the data to a common reference frame and temporal resolution.

3.1. Alignment

Every pulse emitted from the neutron star does not arrive simultaneously at different telescopes observing at different frequencies. The main reason for this is the interstellar dispersion, which causes the high frequency radiation of the pulses to arrive earlier, relative to its lower frequency complement. Further variations arise from the different path-lengths to the telescopes. Therefore, in order to align the data from the different telescopes, it is necessary to transform the site arrival time of the radio pulses to a common reference frame. This was chosen to be the pulse arrival time at the solar system barycentre, according to the DE200 ephemeris (Standish 1982). To eliminate dispersion effects, the time of arrival of each pulse was referred to the time of arrival of the pulse at infinite frequency as is standard practice in pulsar timing experiments (see for example Manchester & Taylor 1977 1977).

3.2. Re-binning

The calibrated and aligned EPN-files produced from data obtained at different telescopes were re-binned to a common time resolution (Fig. 3). This is usually the coarsest time resolution among the original files: A common time interval $I_c = [T_{\rm start}, T_{\rm stop}]$ is defined around each pulse, which lies within all individual time intervals $I_i = [t_{\rm start}, t_{\rm stop}]_i$ of the different original data files, such that $I_c \subseteq I_i$, where i denotes each telescope. The common time interval I_c is divided into n_c bins of time length Δt_c. The data contained in all original bins (time length Δt_i), which fall into the time interval of one common bin Δt_c, are then summed up; those which fall only partly into this interval are weighted with the fraction which reaches into Δt_c. Naming the data of the n_c common bins $d_c(j),\ j = 1..n_c$ and the data contained by the n_i original bins $d_i(k),\ k = 1..n_i$, the re-binned data values can be computed through

$$d_c(j) = \frac{\sum_{k=1}^{n_i} d_i(k) \cdot W_j(k)}{\sum_{k=1}^{n_i} W_j(k)} \qquad (1)$$

with $W_j(k) \in [0:1]$ defining the weight of each original bin k as the fraction of it which is contained in the common bin j.

In Fig. 4 an individual pulse of PSR B0329+54 observed at 1.4 GHz in Jodrell Bank is shown. The thin set of lines corresponds to the original data, the thick lines represent the re-binned data. One can see that this procedure affects both the total intensity and the polarization properties to some extent. For instance, changing the effective time resolution has an impact on our ability to detect

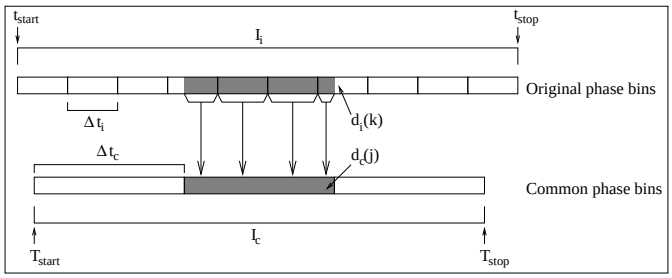

Fig. 3. Procedure to re-bin data to *any* lower time resolution. This method is applied for the analysis of simultaneous observations of individual pulses. See text for details.

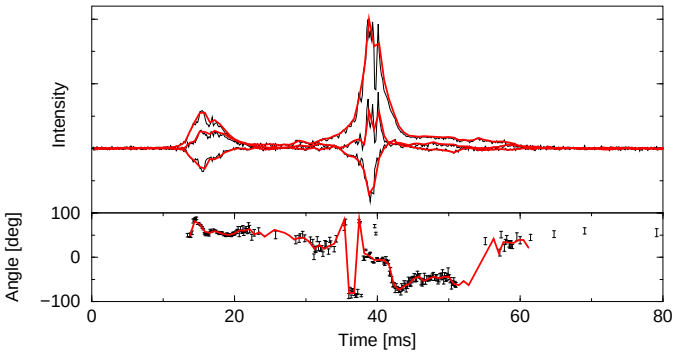

Fig. 4. An individual pulse from PSR B0329+54 in full polarization as observed with the 1.4 GHz receiver in Jodrell Bank (top panel contains total power, linear and circular polarization, the bottom one shows the polarization position angle). The thin lines correspond to the original high time resolution data, the thick lines to the data re-binned to a lower time resolution using the described routine.

OPM jumps (notice the bins just before 40 ms). Such effects have been studied by Gangadhara et al. (1999) and will also be addressed elsewhere (Karastergiou et al. 2001 in prep.). The circular polarization features particularly studied here are at least a few bins wide and therefore the rebinning process does not affect our results. After applying this re-binning technique, the data entries of the corresponding bins can be directly compared.

4. Results

4.1. Cross-Correlation of Phase Bins

In order to study the correlation between the two observing frequencies, we conduct a cross-correlation analysis of the pulse-to-pulse variations of all individual phase bins, following Popov (1986). This yields a two-dimensional correlation array $c_{i,j}$. Each point (i,j) is the correlation coefficient between the time series $f_i(k)$ of bin i at one frequency and the time series $g_j(k)$ of bin j at the other frequency with k being the pulse number. For n pulses, $c_{i,j}$ is obtained through

$$c_{i,j} = \frac{1}{n \cdot \sigma_{f,i} \cdot \sigma_{g,j}} \sum_{k=1}^{n} [f_i(k) \cdot g_j(k) - < f_i >< g_j >] \ , \quad (2)$$

where $\sigma_{f,i}$ and $\sigma_{g,j}$ represent the *rms* deviations of the time series $f_i(k)$ and $g_j(k)$ respectively.
Figures 5 and 6 show contour plots of the correlation arrays for I, L, V and |V|. Those points which fall along the dashed diagonal line represent the correlation array elements $i = j$, i.e. the same phase bins between the two frequencies. The width of the correlated region around the diagonal refers to the time– and spatial scale along which the intensities are correlated. The width is largest for the total power contour plot.

The distribution of the correlation maxima is quite distinct between the different polarizations. In total power (Fig. 5, left plot) three maxima can be identified, which correspond to the three main components of the pulse profile. In linear polarization however (Fig. 5, right plot), the correlation finds its maxima only in the outer components of the profile. Throughout the middle component— which is the strongest also in linear polarization, as can be seen from the integrated profiles on the bottom and the side— the correlation remains significantly lower.

The circular polarization on the other hand shows the opposite characteristic. Regarding the "non-absolute" plot (Fig. 6, left plot), the maximum is clearly situated in the profile centre. It is accompanied by a negative "side maximum" above the diagonal. This corresponds to an anti-correlation which is caused by the sense reversal of the circular polarization often observed at the central component (also seen in Fig. 7). The other "side maximum" expected to be seen beneath the diagonal is not visible due to the selection of contour lines. The outer components are completely uncorrelated. This is mainly caused by heavy frequency dependent fluctuations in these components and especially the opposite handedness, which can be frequently observed (Fig. 7). This can be obviously seen in the analysis of the absolute circular polarization (Fig. 6, right plot), where the difference in handedness is ignored. Some correlation in the outer profile components is now clearly visible.
We note that the results of our cross-correlation analysis are not significantly affected by the number of pulses included in the study. Dividing our sample into sufficiently large sub-samples (for this pulsar a stable integrated profile is obtained after integrating for a few hundred pulses, see Tab. 1 of Helfand et al. 1975) does not change our findings.

4.2. Individual Pulse Pairs

To further investigate specific aspects of the cross-correlation analysis like the disagreement in handedness of the circular polarization, it is often useful to compare individual pulse pairs. Fig. 7 shows two pulse pairs of PSR B0329+54. The overall morphology of the pulses is very similar, especially in total power. However, regarding the polarization characteristics, larger deviations are observed, as revealed by the cross-correlation plots, especially concerning the circular polarization but also the polarization position angle.

- *Polarization position angle (PPA).* Throughout most phases of the pulse longitude, the PPA is consistent between the two frequencies. Yet at some localized phases, significant differences between the PPAs are measured (e.g. arrows in Fig. 7). These differences indicate the simultaneous presence of both orthogonal polarization modes at the two frequencies observed. It is worth noting that the PA difference between the two modes is not always 90^o as noted also by Gil & Lyne (1995) and von Hoensbroech et al. (1998).
  It should again be noted that determining OPMs is affected by the temporal resolution of the observation. It is, therefore, quite significant that we can detect the aforementioned PPA differences after having rebinned our data (as described in §3.2).
- *Circular polarization.* The most prominent differences observed concern the intensity and handedness of the circularly polarized component of the radiation. In the trailing component of the left pulse pair in Fig. 7 a high degree of circular polarization is measured at 2.7 GHz, but none at 1.4 GHz. The cross correlation plot in Fig. 6 indicates that these differences occur preferentially in the outer components, while the central component is well correlated. The fact that the *absolute* circular polarization is well correlated in the outer components indicates a degree of anti-correlation in the circularly polarized power of the outer components. This is explicitly demonstrated in the right pulse pair where the encircled regions show a handedness that is opposite between the two frequencies. Note that the handedness is in fact swapped in both the leading and trailing outer components. At the same time, however, the swing of

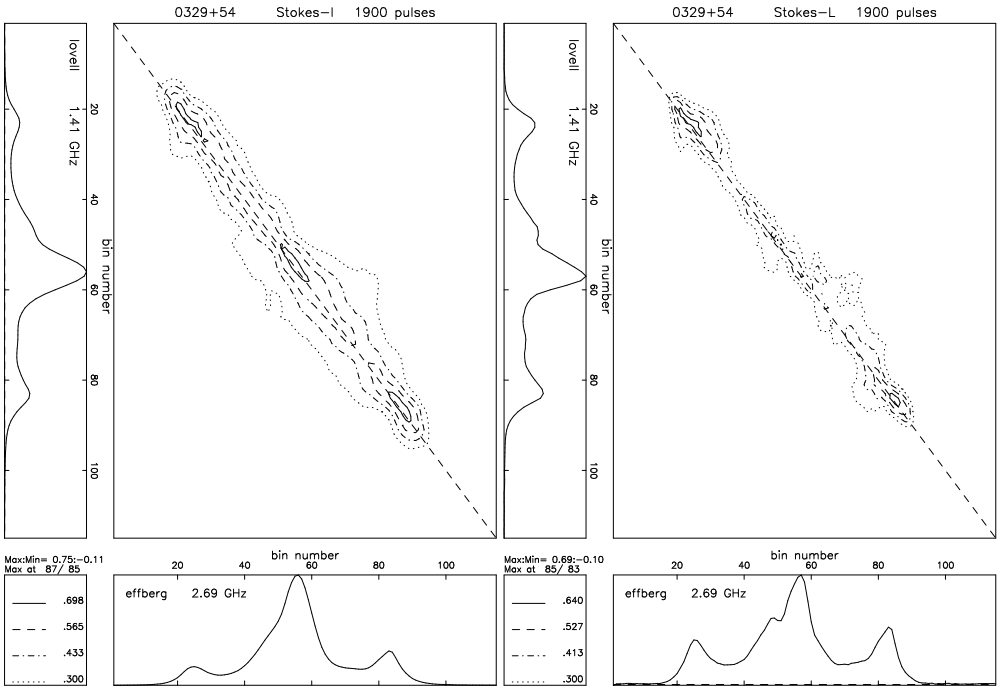

Fig. 5. Contour plot of a bin-by-bin cross correlation function in total intensity (left) and linearly polarized power (right). The pulse-to-pulse fluctuations of each bin at one frequency are correlated against each bin at the other frequency. The profiles in the bottom- and left panel represent the integrated intensities of the respective Stokes parameter. The contour lines correspond to constant correlation coefficients, their representations are plotted in the box on the bottom-left.

the circularly polarized power is identical at the two frequencies for the central component where we see a change from negative to positive handedness.

5. Discussion

We can summarize the results of our analysis as follows:

- the total intensity is well correlated between the two frequencies
- linear polarization is correlated principally in the outer components of the profile
- the two different orthogonal polarization modes can appear simultaneously at the same longitude at different radio frequencies
- in some parts of the profile the sense of circular polarization can change from one frequency to the other while it simultaneously remains unchanged at other parts of the profile

The good total intensity correlation implies that the mechanism responsible for emission at one frequency is also responsible for emission at the other frequency. This strongly suggests that a single event at the bottom of the pulsar magnetosphere is responsible for a sub-pulse observed across the spectrum. This can be explained by a single plasma column streaming along the field lines and radiating with a large bandwidth. This wide-bandwidth picture seems to be in some contradiction to a radius-to-frequency mapping (RFM) model which assumes that the emission at higher frequencies is created closer to the neutron star than that at lower frequencies. The concept of a RFM is mainly based on the observations that pulse profiles become narrower at high frequencies, as expected for pulses emitted in a dipolar magnetic field (Cordes 1975). It also receives support from the observations, that the centre of the PA swing lags the profile midpoint by an amount usually decreasing with frequency, which is interpreted as a decrease in emission height (Blaskiewicz et al. 1991, von Hoensbroech & Xilouris 1997, Hibschman & Arons 2001). For our observations, this apparent conflict, for a frequency dependent emission height and radiation with a bandwidth much larger than the usual observational spacing, can be solved if the particles creating the radiation at separate frequencies are part of the same plasma column.

If the previous assumption is correct, what determines which OPM is emitted at a given frequency? Are OPMs caused by a propagation effect like birefringence? If we accept that pulsar emission is always radiated in two competing modes of polarization, orthogonal to each other (McKinnon & Stinebring 1998), at the same time, then the PA recorded at each pulse phase will have two possible values, separated by $\approx 90^o$. Each set of values forms an S-shaped curve with pulse phase according to the rotating vector model of Radhakrishnan & Cooke (1969), the two curves separated by $\approx 90^o$. Which of the two PA values is observed would then depend solely upon which of the competing modes is stronger at every specific phase.

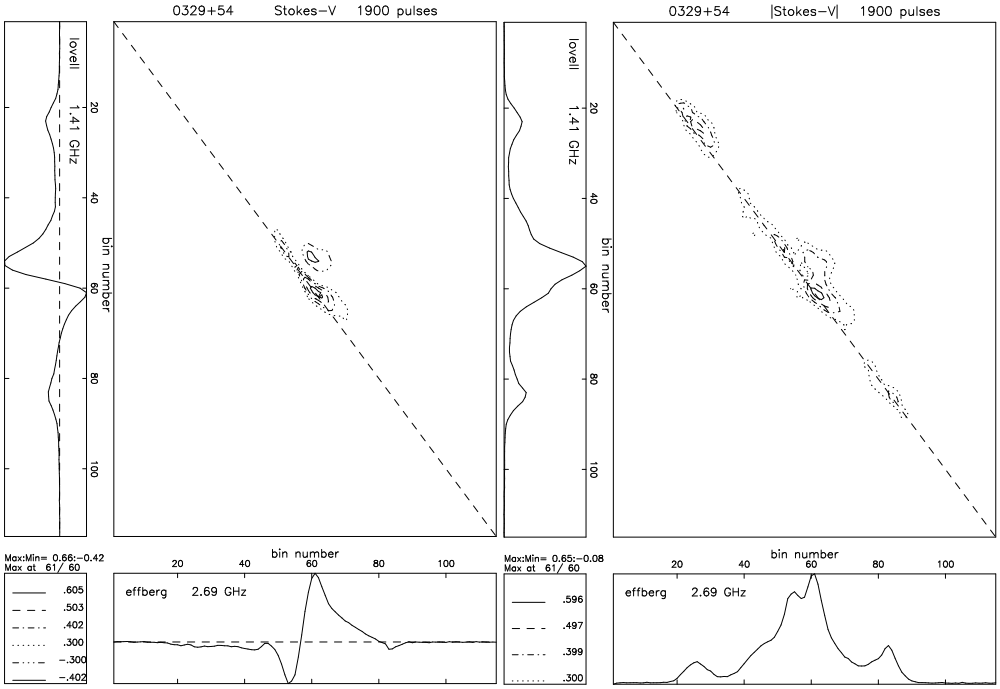

Fig. 6. Contour plot of a bin-by-bin cross correlation function in circularly- (left) and absolute circularly polarized power (right). See caption of Fig. 5 for representations. Note that the little "island" above the diagonal in the left plot corresponds to an anti-correlation, i.e. a disagreement in handedness of the circular polarization. The profile for the absolute circular power is calculated by taking the sum of the absolute circular power of the single pulses and not the absolute of the sum of the circular power of the single pulses. For this reason, the two profiles look somewhat different.

If we could assign a spectral index to the two polarization modes, which may be different, it would be easy to imagine a situation where one mode is dominant at the lower frequency and the other at the higher.

If this scenario of competing OPMs with different spectral indices is correct, the following should be observable: At a particular critical frequency, both modes should be present with almost equal strength and the degree of linear polarization should be ≈ 0. Also, at frequencies at the extreme ends of the observed spectrum on either side of this critical frequency, OPMs would only hardly be observed. Although existing observations by Stinebring et al. (1984) found some increase in the occurrence of OPMs at 1.4 GHz compared to 0.4 GHz, this may not be the general case (Xilouris et al. 1996), and it clearly needs simultaneous observations of the kind presented in this work to study this interesting question in detail. In fact, simultaneous polarimetric observations, at three or more widely spaced frequencies, could possibly reveal a spectral behaviour of the OPMs, also to be investigated in future work.

If the two competing OPMs are created by propagation effects in the pulsar magnetosphere, the polarimetric differences observed at the two frequencies originate from the measured radiation having a slightly different history at the two frequencies. The observed changes in the handedness in circular polarization are hence very intriguing, as they can be indeed most convincingly explained by some propagation effect. A change in the sign of the circular polarization between two frequencies has been observed in the *integrated profiles* of a few pulsars (Han et al. 1998), but seeing this for *individual pulses* clearly demands an explanation. The effect however, seems to be dependent on the pulse longitude, as the central part of the profile is not affected. In the case of PSR B0329+54, the central component is without doubt a core component (Rankin 1983, Lyne & Manchester 1988), which originates from regions near the magnetic axis. Rankin (1990) suggested that core components are emitted from altitudes much lower than those for conal components, implying that the radiation process may be different. Whilst other authors find no evidence for a difference in the radiation mechanism of core and conal components (e.g., Lyne & Manchester 1988, Manchester 1995, Kramer et al. 1999), one would also naively expect that emission from a lower altitude should be more prone to plasma effects as it propagates through the magnetosphere (see von Hoensbroech et al. 1998). That seems to be in contrast to what is observed.

Other factors appear to be more important than simply the radiation's path length before it escapes the magnetosphere. For instance, the magnetic field lines in the core dominated regions have, naturally, a much smaller curvature radius than the conal regions where the observed changes take place. It is therefore very tempting to assume that the location of a given profile longitude mapped on its actual position within the pulsar beam will be an important parameter in the understanding of OPMs

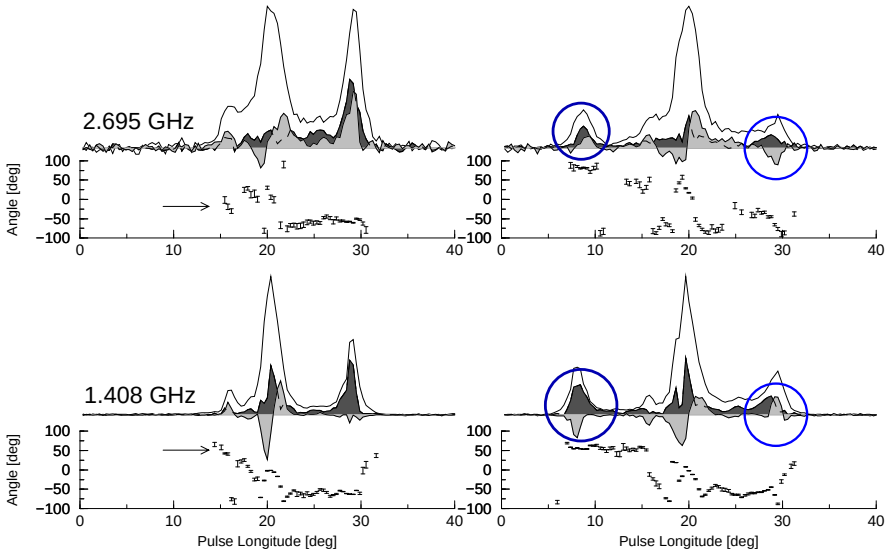

Fig. 7. Two examples of individual pulse pairs of PSR B0329+54, observed in full polarization. The dark-shaded area represents linearly polarized power and the light-shaded area circularly polarized power. The overall correlation is good, but deviations in the polarization are larger than those in the total power. The circular polarization, for example, in the wings of the right pulse pair shows a reversed handedness. Also the arrows in the left pulse pair point to an inconsistency of the PPA between the two frequencies at a specific pulse longitude. Note, also, that only PA points with a significance level of more than 3 σ have been plotted. The pulse components of the higher frequency in the above pulse pairs appear broader. However, this is not the general case, since we also see cases where the higher frequency pulse components appear narrower. This fact raises a question about the spectral indices of pulse components, to be studied in future work.

and propagation effects in the pulsar magnetosphere. Our observations of more pulsars simultaneously at different frequencies can hence provide very valuable insight.

6. Conclusions

The simultaneous observation of individual pulses in full polarization allows an investigation of the instantaneous frequency dependence of a localized emission from the pulsar magnetosphere. The various types of analyses applied reveal mainly one fact: the polarization characteristics of single pulses seem to differ a great deal more than the total power at different frequencies. This can be seen in the direct comparison of individual pulses, but also through various types of cross correlation analyses. It is shown that the correlation between different frequencies is less for the polarized intensities, especially for the circular polarization.

It is clearly shown that the differences in the polarization properties vary between the central and outer components. It seems that the circular polarization is more stable in the central component. In the outer components, the circular polarization sometimes even shows reversed handedness between the two frequencies. This implies that polarization fluctuations at a specific longitude may depend strongly on the curvature of the magnetic field lines at that longitude mapped on its position within the pulsar beam. This, in conjunction with the various paths of the radiation through the pulsar magnetosphere, could be vital in explaining the observed polarization properties.

The quality of the new results presented here underline the necessity of more such observations in the future to confirm the first results, which should establish multi-frequency simultaneous observations as a first-class tool for investigating the emission mechanism of radio pulsars.

7. Future work

The present paper is the first in a series of papers concerning simultaneously observed pulsar data, which focuses on a particular polarimetric experiment between the Effelsberg and Jodrell Bank radio telescopes. Other observing runs, that have been carried out within the frame set of the EPN and coordinated by the pulsar group of the MPIfR in Bonn, will be the subject of papers to follow. These runs mainly consist of total-power, simultaneous observations between the radio-telescopes in Bologna, Westerbork, Torun, Pushchino, Ooty, Effelsberg and Jodrell Bank, and span through a frequency range between 100 MHz (Pushchino) and 5 GHz (Effelsberg). We are expecting more polarimetry associated work in the future with the addition of Westerbork and the GMRT. Further results from data already taken will be published in due course.

Acknowledgements. Simultaneous observations of the radio pulsars studied required a maximum degree of organisation

and cooperation between the parties involved. We would especially like to thank Christoph Lange and Norbert Wex for their assistance in the realization of the project. We would also like to acknowledge the scientists who have participated in the ever growing EPN network, which has at times incorporated the likes of the Pushchino, Ooty and GMRT radio telescopes. We also want to give credit to all the technical staff at the mentioned observatories for making our work as easy and as efficient as possible.

References

Barnard J. J., Arons J., 1986, ApJ 302, 138
Bartel N., Sieber W., 1978, A&A 70, 260
Bartel N., Kardashev N. S., Kuzmin A. D., et al., 1981, A&A 93, 85
Bartel N., Morris D., Sieber W., Hankins T. H., 1982, ApJ 258, 776
Blaskiewicz M., Cordes J. M., Wasserman I., 1991, ApJ 370, 643
Borriakoff V., Ferguson D. C., Slater G., 1981, IAU Symp. No. 95, 199
Davies J.G., Lyne A.G., Smith F.G., et al., 1984, MNRAS 211, 57
Gangadhara R. T., Xilouris K. M., von Hoensbroech, A., et al., 1999, A&A 342, 474
Gil J. A., Lyne A. G., 1995, MNRAS 276, L55
Gould D. M., Lyne A. G., 1998, MNRAS 301, 235
Han J. L., Manchester R. N., Xu R. X., Qiao G. J., 1998, MNRAS 300, 373
Helfand D. J., Manchester R. N., Taylor J. H., 1975, ApJ 198, 661
Hibschman J. A., Arons J., 2001, ApJ 546, 382
Karastergiou A. et al., 2001, A&A, in prep.
Kardeshev N. S., Nikolaev Ya. N., Novikov A. Yu., et al., 1986, A&A 163, 114
Kramer M., 1994, A&AS 107, 527
Kramer M., Jessner A., Doroshenko O., Wielebinski, R., 1997, ApJ 488, 364
Kramer M., Lange Ch., Lorimer D.R., et al., 1999, ApJ 526, 957
Lorimer D. R., Jessner A., Seiradakis J. H., et al., 1998, A&AS 128, 541
Lyne A.G., 1971, MNRAS 153, 27
Lyne A.G., Manchester R.N., 1988, MNRAS 234, 477
Manchester, R.N., 1995, JA&A, 16, 107
Manchester R. N., Taylor J. H., 1977, Pulsars, Freeman, San Francisco
McKinnon M. M., Stinebring D. R., 1998, ApJ 502, 883
Melrose D. B., 1995, JA&A, 16, 137
Melrose D. B., 2000, Pulsar Astronomy - 2000 and Beyond, ASP Conference Series, Vol. 202, 721
Popov M. V., 1986, SOVIET ASTR. 30, 577
Radhakrishnan V., Cooke D. J., 1969, Ap. Letters, 3, 225(RC)
Rankin J. M., 1983, ApJ 274, 358
Rankin J. M., 1990, ApJ 352, 247
Sallmen S., Backer D., Hankins T., Moffett D., Lundgren S., et al., 1999, ApJ 517, 460
Stinebring D. R., Cordes J. M., Rankin J. M., Weisberg J. M., Boriakoff, V., 1984, ApJS 55, 247
Standish, E. M., 1982, A&A 114, 297
von Hoensbroech A., 1999, PhD Thesis, University of Bonn, Bonn
von Hoensbroech A., Lesch H., Kunzl T., 1998, A&A 336, 209
von Hoensbroech A., Xilouris K. M., 1997, A&AS 126, 121
Xilouris K. M., Kramer M., Jessner A., Wielebinski R., Timofeev M., 1996, A&A 309, 481